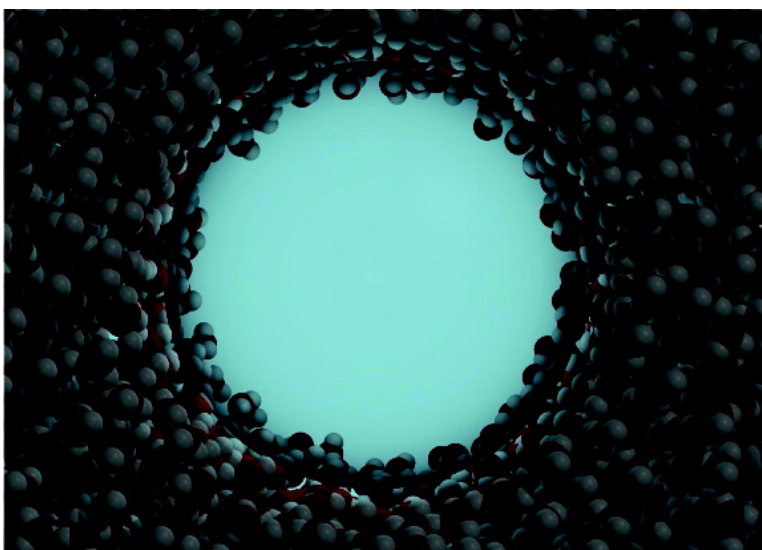


The Collapse of Nanobubbles in Water

Francesca Lugli, Siegfried Hfinger, and Francesco Zerbetto

J. Am. Chem. Soc., **2005**, 127 (22), 8020-8021 • DOI: 10.1021/ja0505447 • Publication Date (Web): 11 May 2005

Downloaded from <http://pubs.acs.org> on March 25, 2009



More About This Article

Additional resources and features associated with this article are available within the HTML version:

- Supporting Information
- Links to the 7 articles that cite this article, as of the time of this article download
- Access to high resolution figures
- Links to articles and content related to this article
- Copyright permission to reproduce figures and/or text from this article

[View the Full Text HTML](#)

The Collapse of Nanobubbles in Water

Francesca Lugli, Siegfried Höfner, and Francesco Zerbetto*

Dipartimento di Chimica "G. Ciamician", Università degli Studi di Bologna, V. F. Selmi 2, 40126 Bologna, Italy

Received January 27, 2005; E-mail: francesco.zerbetto@unibo.it

The coalescence of bubbles bears on several practical aspects,^{1,6} such as propellers erosion, the generation of luminescence, and a special case of chemical reactivity. Bubbles were advocated to drive microfluidic transport, and their presence was reported in atomic force microscopy experiments.⁵ The description of bubble collapse has long been done in terms of hydrodynamics.^{1,6} Information on the collapse⁷ is obtained usually through sonoluminescence experiments.⁸ Theoretically, analytical models² and semianalytic solutions of the dynamics of collapse have appeared,⁹ together with atomistic simulations with simple Lennard-Jones potentials.¹⁰ The appearance of cavities has been studied by molecular dynamics simulations.¹¹ The present molecular dynamics simulations of bubble collapse were performed¹² for the idealized cavity with a radius of 1 nm (an additional calculation was performed for a radius of 1.5 nm) at constant pressure of 1 atm. During the collapse, the system was not coupled to a thermal bath, and temperature was allowed to vary freely. Water was described by the SPC model.¹³ All simulations were carried out with the TINKER package.¹² Bubbles were created inside cubic boxes with up to 3000 water molecules. The systems were equilibrated in the presence of a Lennard-Jones potential at their center with a collision radius of 1 (or 1.5) nm. After equilibration, a minimum of five statistically independent collapses for each radius and each temperature were run. The cavity was divided in at least six concentric shells of equal thickness; the associated radius was reached when the water density inside the shell was half that of the bulk. Figure 1 shows that the collapse time is of the order of ~ 10 ps and is a function of temperature. According to hydrodynamics, if the collapse of the cavity is rapid, that is, *violent*, the radius variation in time is

$$R(t) = R_0 \left(\frac{t_c - t}{t_c} \right)^{2/5} \quad (1)$$

where R_0 is the initial radius, and t_c is the time of collapse that is obtained here by the simulations. Figure 1 also compares our results and the curves obtained with eq 1. The agreement is satisfactory and implies that nanobubble collapse follows the hydrodynamics description in the violent regime at all temperatures of liquid water. A similar trend was found for a bubble of 15 Å radius at 300 K. An increase of temperature of 80 K, from 280 to 360 K, decreases the lifetime of the cavity by more than a factor of 2. To the best of our knowledge, the temperature dependence of t_c has only been explored with simplified models, such as the perfect gas model,^{9c} where it goes as $T^{-0.5}$ and, therefore, has a much weaker dependence than that found by our simulations, where it is either linear with a correlation coefficient, $r = 0.988$, or quadratic with a correlation coefficient, $r = 0.997$ (parameters and their errors are given in the Supporting Information).

We monitored the local temperature of the wall of water molecules pouring into the cavity and found transient local temperatures of several thousand degrees (see Table 1). The table also reports the velocity of collapse of the cavity wall at 99% of

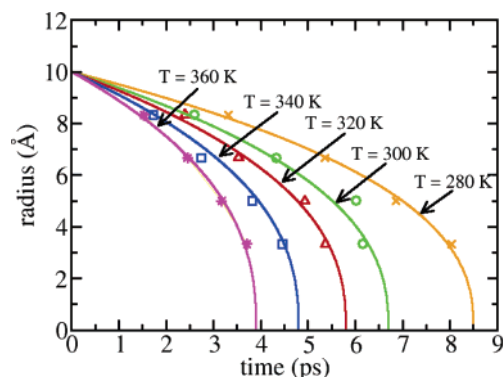


Figure 1. Collapse of cavities in water. The points are obtained using atomistic molecular dynamics and the lines from eq 1, where the time of collapse, t_c , is also determined from the present simulations.

Table 1. Summary of the Calculations of Bubble Collapse in Water^a

T_{bulk} (K)	R_0 (Å)	t_c (ps)	T_{max} (K)	$v_{99\%}$ (m s ⁻¹)	z (ps ⁻¹); c (ps) ^b
280	10	8.5 ± 0.1	1570	750	0.45; 2.09
300	10	6.7 ± 0.1	2180	950	0.56; 1.98
320	10	5.8 ± 0.1	2130	1093	0.62; 1.62
340	10	4.8 ± 0.1	2470	1320	0.83; 1.21
360	10	3.9 ± 0.1	4350	1625	0.86; 1.02
300	15	12.0 ± 0.1	3250	790	0.35; 3.71

^a R_0 is the initial radius; t_c is the collapse time; T_{max} is the maximum temperature achieved during the collapse. For the other parameters, see text. ^b The error on every z is ± 0.01 ; the error on every c is lower than ± 0.03 .

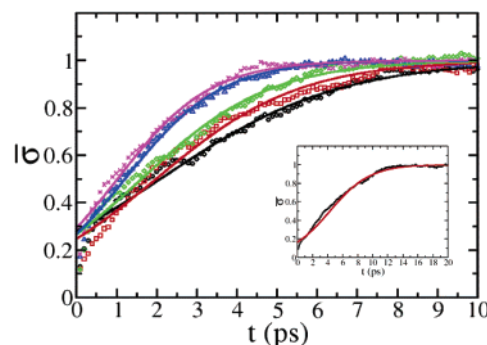


Figure 2. Variation of normalized number density for two cavities of radius 10 and 15 Å (inset) and the fitting with the logistic equation (solid line). Black for 280 K, red for 300 K, green for 320 K, blue for 340 K, purple for 360 K.

the filling, $v_{99\%}$. Experimentally,⁷ for bubbles in the micrometer size domain and at room temperature, it was estimated that $1200 \leq v_{\text{final}} \leq 1600$ m s⁻¹. The present value of $v_{99\%} = 950$ m s⁻¹ is in reasonable agreement. Alternatively to the radius variation, the collapse can be monitored as a function of the number density of water inside the cavity. Figure 2 shows the variation of normalized number density for the two cavities studied here at various

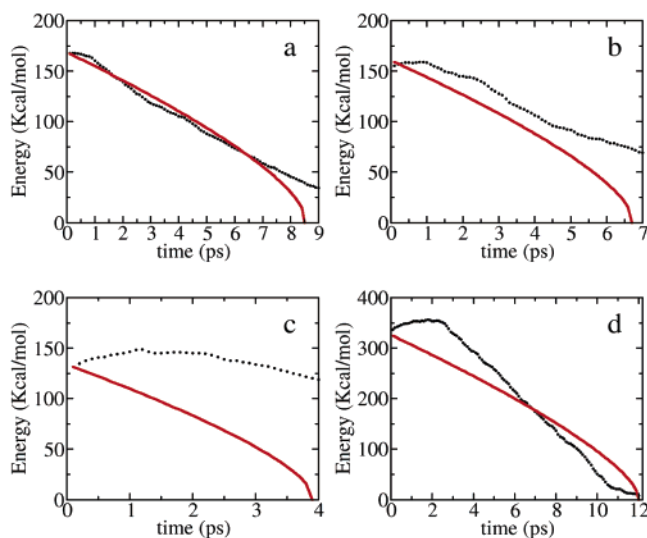


Figure 3. Comparison between $\Delta E = \gamma 4\pi R^2(t) + T\Delta S$ (red line) and the results of molecular dynamics simulations (dotted line) for the energy variation during bubble collapse: (a) $R_0 = 10 \text{ \AA}$, $T = 280 \text{ K}$; (b) $R_0 = 10 \text{ \AA}$, $T = 300 \text{ K}$; (c) $R_0 = 10 \text{ \AA}$, $T = 360 \text{ K}$; (d) $R_0 = 15 \text{ \AA}$, $T = 300 \text{ K}$. The error in the dotted curves is $19.4 \text{ kcal mol}^{-1}$.

temperatures, and the fitting in terms of the solution of the logistic equation that has found wide use to describe the growth of a population in the presence of limiting factors (such as predators for animals). Here, the limiting factor is the number density of water, σ_0 , at the temperature of the simulation. If one normalizes the equation to σ_0 , the logistic equation is

$$\bar{\sigma}(t) = \frac{1}{1 + \exp(-z(t - c))} \quad (2)$$

where z is the Malthusian parameter, proportional to the rate of cavity filling, and c is the time to reach half the limit population.

In an Arrhenius plot, the logarithm of z plotted against the inverse of the temperature yields an activation energy of $1.7 \text{ kcal mol}^{-1}$; the activation energy of self-diffusion of water is $\sim 4.5 \text{ kcal mol}^{-1}$.¹⁴

During the collapse, the energy of the system changes. Macroscopically, a simple description entails the variation of the free energy, ΔF , of the surface in time. Neglecting curvature effects, the free energy of an equilibrated surface cavity is proportional to the area, $4\pi r^2$, multiplied by the surface tension, γ , at each bulk temperature.^{15,16} The use of γ for the bulk is in keeping with the Rayleigh–Plesset equation. If the bubble collapse was a perfectly adiabatic process, the free energy variation could be calculated by combining eq 1 and the surface area, $\Delta F = \gamma 4\pi R^2(t)$. Corrections for the curvature may also be considered.¹⁷ For a comparison with the MD results, one needs the energy $\Delta E = \Delta F + T\Delta S$, where $\Delta S = k_B \ln(0.5)^N$, with N being the number of water molecules in the collapsing wall at every time. The factor of 0.5 is the ratio of hydrogen bonds in the bulk and on the surface.¹⁸ Figure 3 compares

the variation of energy during the collapse calculated using molecular dynamics and the qualitative approach. At low temperatures (280 K), there is good agreement between the two approaches. As the temperature increases, the collapse becomes less and less adiabatic. In particular at 360 K, close to the boiling point, any resemblance between the two approaches is lost. However, at sufficiently low temperatures, the energy variation of the collapse of bubbles in water is rather well described by a simple equation. The main conclusion of this work is that the collapse of nanosize bubbles in water can be monitored in different ways: (1) it follows the simple analytical solution of the Rayleigh–Plesset equation in the violent regime at all temperatures; (2) it satisfies a logistic growth equation of the filling of the cavity until the liquid inside reaches the standard water density; and (3) empirically, at temperatures far from the boiling point, we find that the energy variation during the implosion of the MD runs is well reproduced by combining a qualitative approach.

Supporting Information Available: Some computational and theoretical details.

References

- (1) (a) Brennen, C. E. *Cavitation and Bubble Dynamics*; Oxford University Press: New York, 1995. (b) Philipp, A.; Lauterborn, W. *J. Fluid Mech.* **1998**, *361*, 75–116. (c) Rayleigh, J. W. *Philos. Mag.* **1917**, *34*, 94–98.
- (2) (a) Brenner, M. P.; Hilgenfeldt, S.; Lohse, D. *Rev. Mod. Phys.* **2002**, *74*, 425–484. (b) Webb, S. M.; Mason, N. J. *Eur. J. Phys.* **2004**, *25*, 101–113.
- (3) (a) Suslick, K. S. *Science* **1990**, *247*, 1439–1445. (b) Didenko, Y. T.; Suslick, K. *Nature* **2002**, *418*, 394–397. (c) Lohse, D. *Nature* **2002**, *418*, 381–382.
- (4) Marmottant, P.; Hilgenfeldt, S. *Proc. Natl. Acad. Sci. U.S.A.* **2004**, *101*, 9523–9527.
- (5) (a) Ishida, N.; Inoue, T.; Miyahara, M.; Higashitani, K. *Langmuir* **2000**, *16*, 6377–6380. (b) Yang, J.; Duan, J.; Fornasiero, D.; Ralston, J. *J. Phys. Chem. B* **2003**, *107*, 6139–6147.
- (6) (a) Plesset, M. S.; Prosperetti, A. *Annu. Rev. Fluid Mech.* **1977**, *9*, 145–185. (b) Noltingk, B. E.; Neppiras, E. A. *Proc. Phys. Soc. B* **1950**, *63*, 674–685.
- (7) Weninger, K. R.; Barber, B. P.; Putterman, S. J. *Phys. Rev. Lett.* **1997**, *78*, 1799–1802.
- (8) (a) Didenko, Y. T.; McNamara, W. B., III; Suslick, K. S. *J. Am. Chem. Soc.* **1999**, *121*, 5817–5818. (b) Taleyarkhan, R. P.; West, C. D.; Cho, J. S.; Lahey, R. T., Jr.; Nigmatulin, R. I.; Block, R. C. *Science* **2002**, *295*, 1868–1873.
- (9) (a) Bogoyavlenskii, V. A. *Phys. Rev. E* **1999**, *60*, 504–508. (b) Bogoyavlenskii, V. A. *Phys. Rev. E* **2000**, *62*, 2158–2167. (c) Rickayzen, G.; Powles, J. G. *Mol. Phys.* **2002**, *100*, 3823–3828.
- (10) Xiao, C.; Heyes, D. M.; Powles, J. G. *Mol. Phys.* **2002**, *100*, 3451–3468.
- (11) (a) Pratt, L. R.; Pohorille, A. *Proc. Natl. Acad. Sci. U.S.A.* **1992**, *89*, 2995–2999. (b) Pratt, L. R. *Annu. Rev. Phys. Chem.* **2002**, *53*, 409–436.
- (12) (a) Ponder, J. W.; Richards, F. J. *J. Comput. Chem.* **1987**, *8*, 1016–1024. (b) Kundrot, C.; Ponder, J. W.; Richards, F. J. *J. Comput. Chem.* **1991**, *12*, 402–409. (c) Dudek, M. J.; Ponder, J. W. *J. Comput. Chem.* **1995**, *16*, 791–816.
- (13) Berendsen, H. J. C.; Postma, J. P. M.; van Gusteren, W. F.; Hermans, J. In *Intermolecular Forces*; Pullmann, B., Ed.; Reidel: Dordrecht, The Netherlands, 1981.
- (14) Mills, R. J. *Phys. Chem.* **1973**, *77*, 685–688.
- (15) (a) Hoefinger, S.; Zerbetto, F. *J. Phys. Chem. A* **2003**, *107*, 11253–11257. (b) Hoefinger, S.; Zerbetto, F. *Chem.–Eur. J.* **2003**, *9*, 566–569.
- (16) Vargaftik, N. B.; Volkov, B. N.; Voljak, L. D. *J. Phys. Chem. Ref. Data* **1983**, *12*, 817–820.
- (17) Barrett, J. C. *J. Chem. Phys.* **2004**, *120*, 7636–7642.
- (18) Dill, A. K.; Bromberg, S. *Molecular Driving Forces*; Garland Science: New York, 2003; pp 580–582.

JA0505447